# 铀酰叠氮离子化合物的质谱分析与理论计算

洪 静[1,2],韩昌财[3],费泽杰[1],唐圆圆[1],刘艳成[1],
周露露[4],刘洪涛[1],熊孝根[5],董常武[1,*]

1. 中国科学院 上海应用物理研究所,上海 201800;
2. 中国科学院大学,北京 100049;3. 同济大学 化学科学与工程学院,上海 200092;
4. 山东能源集团有限公司,山东 济南 250101;5. 中山大学 中法核工程与技术学院,广东 珠海 519082

**摘要**:铀的多配位化学不仅在新型锕系化合物的结构研发中具有重要地位,也对环境和核废料处理问题产生重要影响。本研究报道了激光溅射 U 靶在 $N_2O$ 载气中冷却膨胀生成$[UO_2(N_3)_n]^+$($n$=0—4)的质谱结果,并结合理论计算对所生成离子的稳定结构和成键相互作用进行了分析。结果显示,$N_3$ 以自由基的形式与 $UO_2^+$ 配位,且第一个 $N_3$ 配体与 $UO_2^+$ 存在成键相互作用。此外,进一步的定域化分子轨道分析表明,体系中存在多中心轨道离域。

**关键词**:锕系配位化学;铀酰化合物;计算化学;叠氮自由基化合物
**中图分类号**:TL211.3;O657.63 **文献标志码**:A **文章编号**:0253-9950(2023)05-0466-11
**doi**:10.7538/hhx.2023.45.05.0466

# Mass Spectrum and Theoretical Calculation for Azide Radical Complexes With Uranyl(Ⅵ) Cation $[UO_2(N_3)_n]^+$($n$=1-4)

HONG Jing[1,2], HAN Chang-cai[3], FEI Ze-jie[1], TANG Yuan-yuan[1], LIU Yan-cheng[1],
ZHOU Lu-lu[4], LIU Hong-tao[1], XIONG Xiao-gen[5], DONG Chang-wu[1,*]

1. Key Laboratory of Interfacial Physics and Technology, Shanghai Institute of Applied Physics, Chinese Academy of Sciences, Shanghai 201800, China;
2. University of Chinese Academy of Sciences, Beijing 100049, China;
3. School of Chemical Science and Engineering, Tongji University, Shanghai 200092, China;
4. Shandong Energy Group Co,. LTD, Jinan 250101, China;
5. Sino-French Institute of Nuclear Engineering and Technology, Sun Yat-sen University, Zhuhai 519082, China

**Abstract**: Coordination of uranium chemistry by multiligands has attracted attention as a way to obtain unique molecular structures and their possible use in environmental and nuclear waste disposal. In this work, mass spectrum with positive ions $[UO_2(N_3)_n]^+$($n$=0-4) as the dominant peaks generated by laser evaporation of uranium target with $N_2O$ as the carrier

**收稿日期**:2022-12-29;**修订日期**:2023-03-21
**基金项目**:国家自然科学基金(22004128, 22273121);中国科学院青年创新促进会基金(2021255);中国科学院上海应用物理研究所"育新计划"(E0553201);中国科学院战略性先导科技专项(XDA02020000);山东省重点研发计划(重大科技创新工程)(2020CXGC010402);广州市科技计划项目(202102080374)
* **通信联系人**:董常武

gas is reported. The associated quantitative calculations are carried out to explore structures and bonding interactions. The calculations show that $N_3$ is bound to $UO_2^+$ as a radical and reveal that the bonding interaction in the whole system is found only between the first $N_3$ ligand and uranium atom. Further localized molecular orbital analyses indicate the presence of multi-centered orbital delocalization in the system.

**Key words**: actinide coordination chemistry; uranyl complexes; computational chemistry; azide radical complexes

Due to the involvement in reprocessing and long-term storage of nuclear fuel, actinide coordination chemistry has a fundamental impact on the energy and environmental issues[1]. Knowledge of the structures, bonding, and reactivities of the actinide complexes reveals the intrinsic role of 5f-element chemistry and provides a foundation for predicting and manipulating their physical and chemical behavior. Urany(Ⅵ), as the most dominant species of uranium in the environmental conditions, has attracted great attention[2-3]. Urany(Ⅵ) is commonly known to have a linear electronic ground state with a closed shell configuration $^1\Sigma_g^+$ and readily bind ligands on its equatorial plane[4]. Spectroscopic investigations of $UO_2^{2+}$ complexes in the gas phase and in solution have been widely discussed[5-10]. It has been reported that $UO_2^{2+}$ typically has saturated 4-6 ligands in the condensed phase[11-12], while it tends to maintain a relatively low coordination number in the gas phase owing to the increased coulomb repulsion between ligands. Despite its inherent stability, uranyl(Ⅵ) can undergo many transformations in the environment. For example, it can be reduced from soluble uranyl(Ⅵ) to insoluble $U^{4+}$. Such transformation is considered to proceed by a disproportionation mechanism so that the formation of another valence form of pentavalent uranyl(Ⅴ) species is also included. The pentavalent $UO_2^+$ not only acts as an important intermediate in the precipitation of uranium from groundwater, but also often as a redox transition product of $UO_2^{2+}$ in photocatalysis and photochemistry. However, there is a paucity of electronic structure and coordination information studies on $[U^VO_2]^+$. This can be mainly attributed to its low stability in water, which is manifested in its tendency to disproportionate into tetravalent and hexavalent uranium species in an aqueous environment[13]. Due to the essential transition state characteristics of $UO_2^+$, the investigation of its associated coordination structure and uranium-ligand interactions can provide a basis for predicting its chemical-physical behavior and designing the synthesis of novel uranyl complexes[14-15].

Computational chemistry studies of actinides which are of more practical importance than the tricky experimental explorations due to radioactivity also face major challenges, mainly arising from the special structure of the actinides, as manifested in the combined effects of relativity and electronic correlations, along with the large number of electrons that need to be taken into account owing to the excessive size of the system and the dense manifold of low-lying states[4, 16-17]. Even so, selected uranium complexes have been studied to explore the electronic structure and coordination patterns, mostly in terms of the influence of the ligand on its U-$O_{yl}$ (uranyl) bond distance, U-$O_{yl}$ stretching frequency and electron transfer between uranium-ligand, which can be used as sensitive indicators of the strength of the interaction between uranium and ligand in the equatorial plane[18]. In the theoretical electronic structure study of $UO_2^+$ and $[UO_2(CO_3)_3]^{5-}$ carried out by Ruipérez et al[19], the structure of $[UO_2(CO_3)_3]^{5-}$ was described as a hexagonal bipyramidal with three carbonate ligands coordinated in the equatorial plane, representing a symmetry of $D_{3h}$. The U-$O_{yl}$ bond length in the carbonate complex(1.898 Å,

1 Å=0.1 nm) was calculated to be significantly longer than that of the bare ion (1.742 Å), which was attributed to the reduced electron population in the σ and π bonding orbitals of U-$O_{yl}$. The same occurred in the theoretical study of Páez-Hernández for $[UO_2(CO)_5]^+$ [20], where $[UO_2(CO)_5]^+$ was calculated with complete active space wave-function based *ab-initio* methods. In their results, in addition to increase of the uranyl bond length compared to the bare ion, there is an atypical CO stretching blueshift, which is in contrast to the redshift in transition metal carbonyls, due to the fact that there is no open d shell in $[UO_2(CO)_5]^+$ but only a single f-electron, resulting in an ineffective π-type back-donation from the metal to the ligand.

The exploration of equatorial coordination number $CN_{eq}$ is also one of the points of interest. Meanwhile, the rise of uranium nitride as a new type of nuclear fuel has attracted a lot of attention, U-N bonding interactions have also aroused extensive exploration. In the study on $[NU^{VI}O]^+$ by Zhao et al.[21], a series of complexes with $[NU^{VI}O]^+$ cations as the core and $N_2$ as the equatorial ligand were synthesized in the gas phase. The complete spatial saturation of the linear $[NU^{VI}O]^+$ at an equatorial coordination number of 5, that is $[NUO(N_2)_5]^+$, was confirmed by mass spectrometry-selected infrared photodissociation spectroscopy and quantum chemical calculations. Nevertheless, in Marks' photodissociation and infrared spectroscopy investigation of $U^+(N_2)_n$ complexes, the saturated coordination complex was predicted to be $U^+(N_2)_8$ with a cubic structure[22].

In this work, we report the observation of a series of $[UO_2(N_3)_n]^+$ ($n$=0-4) mass spectral peaks which are produced by laser vaporization of uranium in a pulsed supersonic expansion of $N_2O$ on mass spectrometry for the first time. The structures and the ligand coordination patterns of the obtained series of ion peaks are simulated and discussed through the theoretical calculations. Although this is our first observation of $UO_2(N_3)_n^+$ cations in the gas phase, a series of uranium oxoazides of neutral molecules and anions ($UO_2(N_3)_2$, $[UO_2(N_3)_3]^-$, $[UO_2(N_3)_4]^{2-}$) were previously prepared by the Haiges group[23], who is dedicated to the synthesis and characterization of metal polyazides from the perspective of the stability of azide containing compounds. Azide ions have similar electronegativity and structure to halogen atoms, so they are also known as halogen-like ions. However, the presentation of the ligand and coordination pattern are quite different here. The aim of this article is set to investigate the coordination structure of $[UO_2(N_3)_n]^+$, and to attempt to elucidate the coordination patterns in comparison with previous studies, as well as the effect of ligands on the $UO_2$ unit. The characteristics of uranium-nitrogen bonding will also be discussed.

## 1 Experimental

$UO_2^+$ cations and their $N_3$-ligated complexes were produced by a laser vaporization of a uranium target in the presence of a mixed carrier gas (5%$N_2O$+95%He). A Nd: neodymium-doped yttrium aluminium garnet(YAG) laser fundamental beam(1 064 nm, 10 Hz repetition rate) was focused to form a 1 mm diameter spot on the rotating uranium target. The cluster cations were cooled and expanded into the acceleration field chamber and then extracted perpendicularly by a high pulsed voltage within the accelerating field into a homemade time-of-flight(TOF) mass spectrometer for detection and characterization. The apparatus have been previously described elsewhere[24]. The results of the mass spectrometric analysis are presented in Fig. 1, with $m/z$ in the range of 200-500. The mass spectrum is dominated by the $UO_2^+$ cation and its $N_3$ ligated complexes $[UO_2(N_3)_n]^+$ ($n$=1-4), accompanied by a series of peaks of relatively low intensity and possibly containing hydrogen elements, which also have the same mass difference value of 42 and will not be discussed here. The decreasing intensity of the peaks with increasing mass

number symbolizes the progressive saturation of the coordination. Since the complexes with $N_3$ ligand number greater than 5 were not observed on the mass spectrum, we infer that the $UO_2^+$ complexes saturate at an equatorial ligand number of 4.

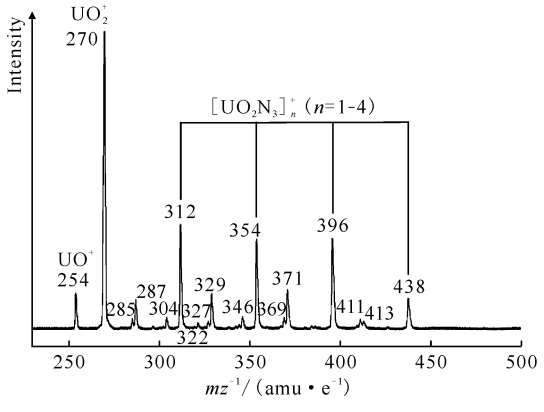


$m/z$ range: 200-500 amu/e

Fig. 1　Mass spectrum of the cluster cations formed by pulsed-laser vaporization of a uranium target in an expansion of nitrous oxide gas

## 2　Calculational

DFT calculations using the Gaussian 09 software packages[25] were carried out on the geometries, vibrational frequencies, and electronic structures of the title complexes by the hybrid density functional B3LYP (Becke three-parameter hybrid functional combined with Lee-Yang-Parr correlation functional)[26]. The vibrational frequency analysis calculations was also performed at the same level of theory to confirm the obtained structures to be true minima. The correlation-consistent triple-ξ (cc-pVTZ) basis sets were employed for N and O atoms[27], and the scalar-relativistic (SR) effective small-core potential ECP60MDF and the corresponding correlation-consistent polarized triple-ξ basis sets (cc-pVTZ-PP)[28-29] were used for U atom. For convenience, we will call the basis sets used in this study as VTZ-PP hereafter. The ligand bonding energies were carried out for the formation of the reactions $[UO_2]^+ + nN_3 \rightarrow [UO_2(N_3)_n]^+ (n=1\text{-}4)$.

The bond order analyses, including Mayer, Wiberg and Fuzzy methods were performed using the Multiwfn software package[30]. We also used the NBO 7.0 program[31] to carry out the natural population analysis(NPA), NBO spin analysis and natural localized valence MO (NLMO) analyses to illustrate the bonding properties between the uranyl unit and the ligands.

## 3　Results and discussion

### 3.1　Geometric structure of $UO_2^+$ and $[UO_2(N_3)_n]^+$ ($n$=1-4)

DFT calculations by SR-B3LYP methods have been performed to predict the geometries for the $[UO_2(N_3)_n]^+$ ($n$ = 1-4) complexes and the isolated $UO_2^+$ cation. The most stable isomers of $[UO_2(N_3)_n]^+$ ($n$=1-4) clusters in each reasonable spin state are presented in Fig. 2 and the cartesian coordinates for stable isomers are listed in Table S1-S6 (See the CNKI enhancement document for details). For the isolated $UO_2^+$, which has been considered as a bare uranyl(Ⅴ) ion[19], the uranyl(Ⅴ) optimal bond length is 1.76 Å, and is about 0.05 Å longer than that in uranyl(Ⅵ)[32-33]. The main reason could be the reduction of the population in the bonding orbitals of uranyl(Ⅴ) due to the repulsion of the extra electron in the 5f orbital of uranium. Like the uranyl(Ⅵ), the pentavalent uranyl has a linear conformation, representing a $C_{\infty v}$ symmetry with electronic configuration of $^2\Phi_u$.

When the first $N_3$ ligand(L1, $^2\Pi_g$) is coordinated on the equatorial plane of $UO_2^+$, the closed-shell $[UO_2N_3]^+$ is formed. And the linear structure of uranyl is weakly bended, as shown in Fig. 2, the angle of the OUO becomes 166°, displaying a $C_{2v}$ symmetry with electronic configuration of $^1A_1$. The bending can be attributed to the steric effect between O atom and $N_3$ group and strong U-N interaction. In the $[UO_2N_3]^+$, the extra 5f electron in U atom and 2p electron in N atom can form a chemical bond and the oxidation state of U is changed from Ⅴ

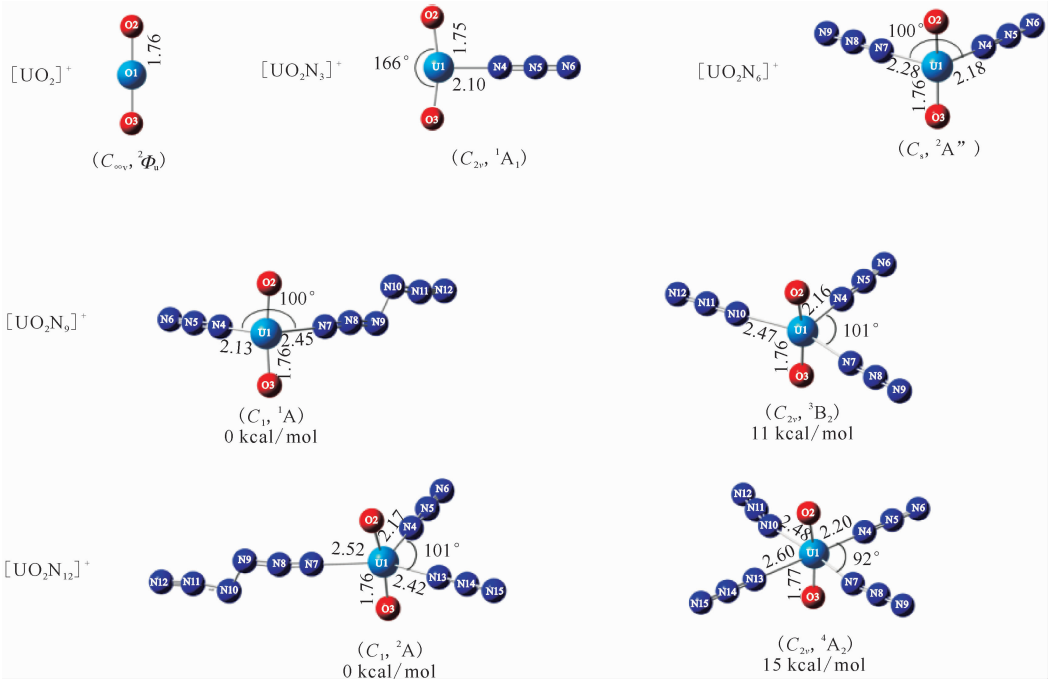


1 cal=4.187 J

The relative energies(kcal/mol), bond length(Å) and bond angle(°) are also given

Fig. 2 Optimized geometries, symmetries and electronic configurations for the ground state $UO_2^+$ and $[UO_2(N_3)_n]^+$ ($n$=1-4) calculated at the SR-B3LYP/VTZ-PP level

to Ⅵ, since the $N_3$ radical can be considered as an electron-withdrawing group. Meanwhile, the U-O bond length is shortened by 0.01 Å compared with that of isolated $UO_2^+$. The U-L1(U1-N4) bond length is calculated to be 2.10 Å, which is much shorter than the sum of single-bond covalent radii for the U and N elements (2.41 Å given by Pyykkö[17]), implying the strong interactions of $UO_2^+$ with L1.

The $[UO_2N_6]^+$ is calculated as the second $N_3$ ligand(L2) continues to be coordinated to U on the equatorial plane. The most stable structure is obtained showing the $^2A''$ ground state with $C_s$ symmetry. The U-L2 (U1-N7) bond length is calculated to be 2.28 Å, which is also shorter than the sum of single-bond covalent radii for the U and N elements. Meanwhile, as the L2 coordinated to U, the U-O and U-L1 bond length are all slightly weakened and elongated by 0.01 Å and 0.08 Å, respectively.

For $[UO_2N_9]^+$, both of the singlet and triplet complexes are calculated and the most stable configurations are obtained with $C_1$ and $C_{2v}$ symmetries in $^1A$ and $^3B_2$ states, respectively. And the singlet isomer is more stable than the triplet one by 11 kcal/mol. As shown in Fig. 2, for the singlet cluster, the third $N_3$ ligand(L3) is linked to the tail of L2 and gives a closed-shell complex, there are still two groups coordinated on the equatorial plane of $UO_2^+$. The U-L1 and U-L2 bond length are calculated to be 2.13 Å and 2.45 Å, respectively. For the triplet cluster, it is a continuation of the previous equatorial coordination model, where L3 is coordinated to U atom. In this isomer, the U-L1 bond length is 2.16 Å and the equally U-L2 and U-L3 (U1-N10) bond length are given to be 2.47 Å. In $[UO_2N_9]^+$, both of U-L2 and U-L3 bond length are exceed the sum of single-bond covalent radii for the U and N elements, implying the weak interactions of $UO_2^+$ with L2 and L3 ligands.

Naturally, for $[UO_2N_{12}]^+$, both of the doublet and quartet complexes are calculated and the most stable configurations are obtained with $C_1$ and $C_{2v}$ symmetries in $^2A$ and $^4A_2$ states, respectively. And the energy of doublet isomer

is determined to be lower than the quartet one by 15 kcal/mol. In both of the two isomers, the fourth $N_3$ ligands(L4) are all coordinated on the equatorial plane of $UO_2^+$, and give rise to the increasing of bond distance between U atom and other $N_3$ ligands.

### 3.2 Equatorial coordination

Throughout the previous studies, the equatorial coordination numbers of ions with uranium atoms as central atoms span a wide range. The series represented by halogenated uranyl complexes[7, 34-35] have the same coordination number $CN_{eq}=4$ as in the present work; the ligands of the $CN_{eq}=5$ complexes include CO, $H_2O$ and some rare gas atoms[20, 36-40]. Some of the smaller rare gas atoms(Ne, He)[38] can reach larger coordination numbers such as $CN_{eq}=6$; further up there are complexes with pure naked uranium atoms $U^+$ as the central ion, where there is an octa-coordination of $CN_{eq}=8$ in the case of CO and $N_2$ ligands[22, 37]. This can be explained by the parameter $Q$, defined as the ratio of the "ligand van der Waals diameter" to the "bond length of center to ligand"[21], which symbolizes the limitation of the coordination number by the size of the ligand space. The dependence between $Q$ and $CN_{eq}$ can be expressed as $Q\leqslant 1$ for $CN_{eq}=6$; $Q\in(1.1,\ 1.2)$ for $CN_{eq}=5$; $Q\geqslant 1.2$ for $CN_{eq}=4$. In this paper, the $N_3$ radical van der Waals diameter is determined to be about 3.5 Å and the distance between $N_3$ radical and U atom is taken as the average of the U-N bond length, which is 2.438 Å, so that the value of $Q$ is $3.5/2.438=1.44$, which is greater than 1.2, providing an explanation for the $CN_{eq}=4$ of $[UO_2(N_3)_4]^+$ with $N_3$ radical as the ligand. Interestingly, in the structure optimization, cluster with $N_6$ ligand is also obtained and the energy is slightly lower than that with pure $N_3$ ligands. According to the judgement about parameter $Q$, the van der Waals diameter of $N_6$ should be much larger than 3.5 Å, thus the $Q$ should be even larger than 1.44. That means the mass signals of $n>4$ for $[UO_2(N_3)_n]^+$ clusters should be observed in the experiment. However, the mass spectra shows that no complex ions with $n>4$ are produced, so it is reasonable to assume that saturation coordination has been reached at $[UO_2(N_3)_4]^+$ with $N_3$ radical as the ligand. And the discussion below will only consider the equatorial coordination model with $N_3$ as the ligand rather than $N_6$.

The stable positions of the four $N_3$ ligands are more or less symmetric at the equatorial plane of $UO_2^+$. The coordination energies are also evaluated under SR-B3LYP/VTZ-PP level. As shown in Fig. 3(a), the total ligand-bonding energies are more negative as the coordination number increasing, implying that each of ligands can stabilize the cluster. Fig. 3(b) illustrates the increasingly weak binding of the newly ligated $N_3$ to U as the coordination number increasing.

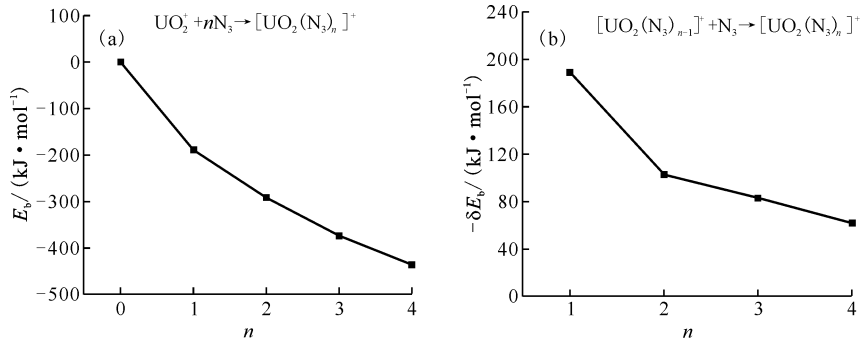


(a): Total ligand-bonding energy $E_b=E([UO_2(N_3)_n]^+)-E(UO_2^+)-nE(N_3)$($n$=0-4);

(b): Differential bonding energy of the last additional $N_3$ ligand($\delta E_b=E([UO_2(N_3)_n]^+)-E([UO_2(N_3)_{n-1}]^+)-E(N_3)$ ($n$=1-4))

Fig. 3　The coordination energies of $[UO_2(N_3)_n]^+$ *vs.* equatorial coordination number $n$=0 or 1 to 4

The $\delta E_b$ of L1 is much larger than others since it forms the U-L1 chemical bond.

### 3.3 Bond distances of U-O and U-N bonds

We are also interested in a systematic view of the effect of ligands on the $UO_2^+$ unit. Exploring the regularity of the changes in the structural parameters of $UO_2^+$ as the number of ligands increases is of great informative importance for regulating the properties of these complexes. For better visualization, the trends of the U-O and U-N bond lengths as the number of ligands changes are plotted and shown in Fig. 4. Beforehand, it should be noted in advance that the $N_3^-$ monocharged anion is a relatively stable negative ion, so the $N_3$ radical shows a strong electron-withdrawing feature. Therefore, it is believed that when the first $N_3$ radical is ligated, the chemical valence of the central atom uranium is oxidized from the pentavalent to hexavalent. And for $[UO_2(N_3)_n]^+$ ($n$=2-4), $N_3$ is bound on the equatorial plane on the basis of $[UO_2N_3]^+$ and the valence of uranium stays in the saturated hexavalent state. This makes the variation of the U-O bond length in Fig. 4(a) well understandable. The change in oxidized state of U atom at the time of binding the L1 leads to an increase in the interaction between the uranium and oxygen atoms, which is reflected in a shortening of the bond length. When the number of ligands exceeds one, the oxidized state of uranium remains the +6, resulting in a weakening of the U-O bond and a progressive lengthening of the bond length. This is similar to the trend in the $[NUO(N_2)]^+$ system where the U-O bond length increases with the number of coordinated $N_2$[21].

The situation of the U-N bond is somewhat special. The discussion here is divided into two cases due to the discrepancy of the $N_3$ coordination patterns. The first one is the U-L1 bond length, which is the U-N bond length in $[UO_2N_3]^+$, as summarized in Fig. 4(b). The bond length variation of the U-L1 bond is not monotonic, which will be explained in the following discussion section. The second one is the dative bond between U and Ln when $n \geqslant 2$. The pattern of action here is distinguished from the azido-metal bond of L1, instead in a dative character. This U-N bond length is named as U-L and is averaged here for convenience in the cases of $n$=2, 3, and 4 each. The average U-L bond length variation is consistent with the U-N bond length variation in the $[NUO(N_2)]^+$ system, as shown in Fig. 4(c)[21]. This can be attributed to two reasons: (1) The unpaired electrons on $N_3$ radicals enter the empty f orbitals of U when the $N_3$ ligands are ligated, which leads to an increase in the populated electrons. These electrons may have a certain shielding effect, resulting in a reduced interaction between the U atom and the ligand. (2) As the ligand increases, the narrowing of the coordination space induces a steric effect, which also leads to the growth of the U-N bond.

### 3.4 NPA charge and NBO spin analyses

The calculated NPA charges of each unit for different number of ligands are listed in Table 1. The uranium atoms show a decreasing trend in the number of positive charges. This can be

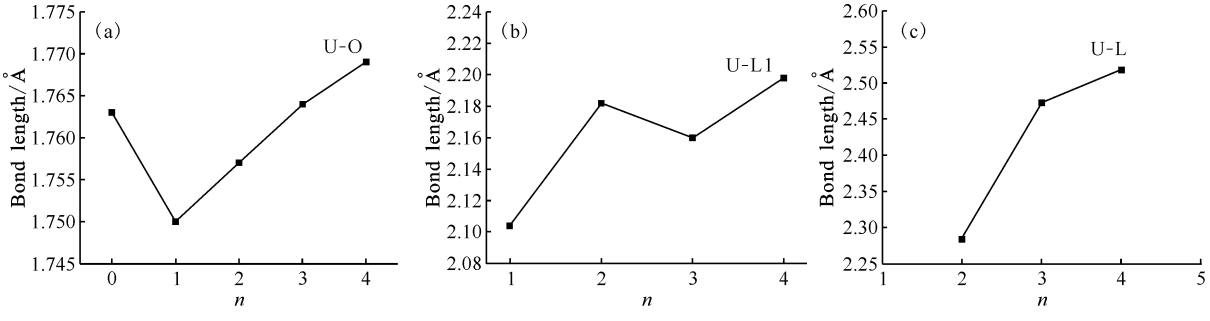


Fig. 4 The bond lengths of U-O(a), U-L1(b) and average bond lengths of U-L(c) *vs* coordination number $n$

Table 1　The NPA charges for $[UO_2(N_3)_n]^+$ ($n$=1-4) and isolate $UO_2^+$ at B3LYP/VTZ-PP level

| Species | NPA charges | | | | | |
|---|---|---|---|---|---|---|
| | U | O | $[N_3]$L1 | $[N_3]$L2 | $[N_3]$L3 | $[N_3]$L4 |
| $UO_2^+$ | 2.106 | −0.553 | | | | |
| $[UO_2N_3]^+$ | 1.980 | −0.389 | −0.202 | | | |
| $[UO_2N_6]^+$ | 1.761 | −0.360 | −0.080 | 0.039 | | |
| $[UO_2N_9]^+$ | 1.614 | −0.379 | −0.150 | 0.147 | 0.147 | |
| $[UO_2N_{12}]^+$ | 1.444 | −0.384 | −0.124 | 0.140 | 0.140 | 0.171 |

accounted for the fact that as the number of ligands increases, unpaired electrons from the $N_3$ radical continuously enter the empty 5f orbitals of the U, leading to an increase in the electron density of the uranium atom. The charge on the oxygen atom changes significantly from $UO_2^+$ to $[UO_2N_3]^+$ and then plateaus later, which is consistent with the valence state of U going from pentavalent uranyl to hexavalent uranyl and then remains constant.

Table 2 provides the results of the NBO spin analysis. It is indicated that $UO_2N_3^+$ is an ion with a closed shell and the electron spin of each atom is 0. And when the additional $N_3$ continues to coordinate to the uranium atom, the electron spin of the previously based $[UO_2N_3]^+$ unit remains essentially constant at values close to zero. This illustrates that the coordination of $N_3$ does not affect the U-L1 bonding when $n>1$. Also, as an independent $N_3$ radical, the probability of the single electron distribution on the N atoms at both ends are the same. While when $N_3$ is coordinated, the single electron distribution undergoes such a change that the probability of distributing on the N atom close to the U atom is greater as shown by the larger spin value on the N atom at this position.

Table 2　The NBO spins for $[UO_2(N_3)_n]^+$ ($n$=1-4) and isolate $UO_2^+$ at B3LYP/VTZ-PP level

| Atom | NBO spins | | | | |
|---|---|---|---|---|---|
| | $UO_2^+$ | $[UO_2N_3]^+$ | $[UO_2N_6]^+$ | $[UO_2N_9]^+$ | $[UO_2N_{12}]^+$ |
| U | 1.083 | 0 | −0.155 | −0.131 | −0.146 |
| O | −0.042 | 0 | 0.051 | 0.050 | 0.056 |
| $N_4$ | | 0 | 0.250 | 0.125 | 0.182 |
| $N_6$ | | 0 | 0.190 | 0.098 | 0.140 |
| $N_7$ | | | 0.451 | 0.600 | 0.573 |
| $N_9$ | | | 0.343 | 0.478 | 0.467 |
| $N_{10}$ | | | | 0.600 | 0.573 |
| $N_{12}$ | | | | 0.478 | 0.467 |
| $N_{13}$ | | | | | 0.640 |
| $N_{15}$ | | | | | 0.507 |

### 3.5　Bond order, Kohn-Sham MO and natural localized valence MO(NLMO) analyses

We further carried out the bond order analyses for U-N bonds based on the Mayer, Wiberg and Fuzzy methods, as listed in Table 3. The results of Fuzzy method are much larger than other two methods. The U-O bond orders for all the complexes are in the region of 2-3. The bond orders of $U_1$-$N_4$ are in the region of 1-2, implying that it is an azido-metal bond. The bond orders of another U-N bond(in L2, L3 and L4) are in the region of 0.5-1. The trend of change in bond order of $U_1$-$N_4$ with the increase of coordination number is consistent with the tendency of the $U_1$-$N_4$ bond length.

The occupied Kohn-Sham molecular orbitals (MOs) relevant to interaction between U atom and the ligands($N_3$ radical) are shown in Fig. S1 (See the CNKI enhancement document for details). For $[UO_2N_3]^+$, the two frontier canonical MOs (HOMO and HOMO-1) are π type bonding orbitals in U-N4 bond, and

HOMO-11 is a σ orbital with bonding character in U-N4 bond, which is in a very low energy level. For $[UO_2N_6]^+$, the HOMO represents an antibonding character between the U f and L1 π* orbitals. It is the reason that the U-N4 bond is weaken as the second ligand(L2) coordinates to $UO_2^+$ unit. Another five MOs (HOMO-1, HOMO-2, HOMO-4, HOMO-15, HOMO-17) represent the bonding character in U-N4 and U-N7 bonds. HOMO-4 is a multi-center π type bonding orbital which involves the p orbitals of two N atoms(N4 and N7) and f orbital of U atom. For $[UO_2N_9]^+$, the bonding character is similar with that in $[UO_2N_6]^+$. The multi-center π type bonding orbital also can be found in HOMO-6, which is predominantly of p orbitals of N7 and N10, f orbital of U and less character of p orbital of N4. For $[UO_2N_{12}]^+$, the bonding character is very similar with that in $[UO_2N_9]^+$.

Table 3 The bond order calculation for $[UO_2(N_3)_n]^+$ ($n$=1-4) and isolate $UO_2^+$ at B3LYP/VTZ-PP level

| Species | Bond order | | |
|---|---|---|---|
| | Mayer | Wiberg | Fuzzy |
| $UO_2^+$ | | | |
| $U_1$-$O_2$ | 2.58 | 2.01 | 2.96 |
| $[UO_2N_3]^+$ | | | |
| $U_1$-$O_2$ | 2.52 | 2.16 | 2.97 |
| $U_1$-$N_4$ | 1.62 | 1.16 | 1.92 |
| $[UO_2N_6]^+$ | | | |
| $U_1$-$O_2$ | 2.46 | 2.15 | 2.92 |
| $U_1$-$N_4$ | 1.23 | 0.94 | 1.66 |
| $U_1$-$N_7$ | 0.86 | 0.67 | 1.34 |
| $[UO_2N_9]^+$ | | | |
| $U_1$-$O_2$ | 2.44 | 2.14 | 2.91 |
| $U_1$-$N_4$ | 1.35 | 1.05 | 1.73 |
| $U_1$-$N_7$ | 0.49 | 0.40 | 1.07 |
| $U_1$-$N_{10}$ | 0.49 | 0.40 | 1.07 |
| $[UO_2N_{12}]^+$ | | | |
| $U_1$-$O_2$ | 2.42 | 2.14 | 2.89 |
| $U_1$-$N_4$ | 1.22 | 0.96 | 1.62 |
| $U_1$-$N_7$ | 0.50 | 0.44 | 1.07 |
| $U_1$-$N_{10}$ | 0.50 | 0.44 | 1.07 |
| $U_1$-$N_{13}$ | 0.33 | 0.30 | 0.89 |

For a better understanding of the U-L bonding in $[UO_2(N_3)_n]^+$ ($n$=1-4), the NLMO analyses are conducted. As shown in Table S7(See the CNKI enhancement document for details), for $[UO_2N_3]^+$, the U-N bond is mainly composed of a 2-center σ-valence molecular orbital(13% U + 86% N) and double 2-center π-valence molecular orbitals(14% U + 73% N). For $[UO_2(N_3)_n]^+$ ($n$=2-4), multi-center π-valence types orbitals are found, which also undergo delocalization among the ligands. In addition, the range of delocalization and the degree of delocalization of the multi-center π-valence orbitals have been changing continuously. This caught our attention and provided an explanation for the seemingly irregular variation of the U-L1 bond length mentioned above. According to the results of NLMO analyses, when the second $N_3$ is coordinated, the π orbitals originally located on U-N4 delocalized to the second ligand, forming a 3-centered delocalized system of N4-U1-N7(16% U1 + 47% N4 + 21% N7) with U-N4 percentage of 63%. It can be interpreted that U-N4 acts as a donor, and the π orbital electrons on the bond are delocalized to the π orbital of U-N7(L2) through the central uranium atom, which leads to a decrease of orbital electrons populated in the U-N4 bond, manifested by a weakening of the bond strength and an increase in the bond length. For $[UO_2N_6]^+$, the extent of delocalization continues to spread into a 4-center system U1-N4-N7-N10(11%U1+73%N4+3%N7+3%N10), but the degree of delocalization at this point decreases instead, with the percentage of delocalized electrons in U-N4 rising back to 84% from 63% in $[UO_2N_6]^+$. This leads to an increase in the density of the populated electrons on the U-N4 bond, exhibiting a shortening of the bond length. Finally, after the fourth $N_3$ coordination, the level of delocalization is greater with the delocalized electron fraction of U-N4 drops to 69%, causing another increase in bond length.

## 4 Conclusion

We provide the geometries of the experi-

mentally obtained series of ions $[UO_2(N_3)_n]^+$ ($n$=1-4) with the aid of theoretical calculations. The U-N bond length is used as a probe to investigate the effect of ligands. NPA charge and NBO spin analyses are also used to further elucidate the strength and properties of ligand-metal interactions. It is noteworthy that the multicenter π orbitals undergo different degrees and ranges of delocalization as the number of ligands increases, which is highly correlated with non-monotonic change of U-N bond length. A spatial interpretation of the coordination number $CN_{eq}=4$ is also given. The experimental and computational results of this work enrich the actinide coordination chemistry and provide some preliminary theoretical bases for the uranyl complexes with $N_3$ as the ligand.

**Express one's thanks**: We would like to thank Prof. Weijun Zheng (Institute of Chemistry, Chinese Academy of Sciences) for providing us the NBO 7.0 software.

**References:**

[1] Morss L R, Edelstein N M, Katz J J, et al. The chemistry of the actinide and transactinide elements: Vol. 2[M]. Netherlands: Springer, 2006.

[2] McGlynn S P, Smith J K. The electronic structure, spectra, and magnetic properties of actinyl ions: part Ⅰ: the uranyl ion[J]. J Mol Spectrosc, 1961, 6: 164-187.

[3] Denning R G. Electronic structure and bonding in actinyl ions and their analogs[J]. J Phys Chem A, 2007, 111(20): 4125-4143.

[4] Pepper M, Bursten B E. The electronic structure of actinide-containing molecules: a challenge to applied quantum chemistry[J]. Chem Rev, 1991, 91(5): 719-741.

[5] Denning R G, Snellgrove T R, Woodwark D R. The electronic structure of the uranyl ion[J]. Mol Phys, 1979, 37(4): 1109-1143.

[6] Flint C D, Tanner P A. Luminescence spectrum of $Cs_2UO_2Cl_4$[J]. J Chem Soc, Faraday Trans 2, 1978, 74: 2210-2217.

[7] Su J, Dau P D, Qiu Y H, et al. Probing the electronic structure and chemical bonding in tricoordinate uranyl complexes $UO_2X_3^-$ (X=F, Cl, Br, I): competition between coulomb repulsion and U-X bonding[J]. Inorg Chem, 2013, 52(11): 6617-6626.

[8] Dau P D, Su J, Liu H T, et al. Observation and investigation of the uranyl tetrafluoride dianion ($UO_2F_4^{2-}$) and its solvation complexes with water and acetonitrile[J]. Chem Sci, 2012, 3(4): 1137-1146.

[9] Gorller-Walrand C, De Houwer S, Fluyt L, et al. Spectroscopic properties of uranyl chloride complexes in non-aqueous solvents[J]. Phys Chem Chem Phys, 2004, 6(13): 3292-3298.

[10] Souter P F, Andrews L. Infrared spectra of some uranium oxyfluoride molecules isolated in solid argon[J]. J Mol Struct, 1997, 412(3): 161-167.

[11] Chakravorti M C, Bandyopadhyay N. Fluoro complexes of hexavalent uranium Ⅲ: complexes of the series $[UO_2F_4]^{2-}$[J]. J Inorg Nucl Chem, 1971, 33(8): 2565-2571.

[12] Mak T C W, Yip W H. Synthesis and crystal structure of bis(tetramethylammonium) aquotetra-fluorodioxouranate(Ⅵ) dihydrate, $[(CI_3)_4N]_2[UO_2F_4(H_2O)]\cdot 2H_2O$[J]. Inorg Chim Acta, 1985, 109(2): 131-133.

[13] Faizova R, White S, Scopelliti R, et al. The effect of iron binding on uranyl(Ⅴ) stability[J]. Chem Sci, 2018, 9(38): 7520-7527.

[14] Steele H, Taylor R J. A theoretical study of the inner-sphere disproportionation reaction mechanism of the pentavalent actinyl ions[J]. Inorg Chem, 2007, 46(16): 6311-6318.

[15] Arnold P L, Love J B, Patel D. Pentavalent uranyl complexes[J]. Coord Chem Rev, 2009, 253(15-16): 1973-1978.

[16] Gagliardi L, Roos B O. Multiconfigurational quantum chemical methods for molecular systems containing actinides[J]. Chem Soc Rev, 2007, 36(6): 893-903.

[17] Pyykkö P. Relativistic effects in structural chemistry[J]. Chem Rev, 1988, 88(3): 563-594.

[18] Di Pietro P, Kerridge A. U-$O_{yl}$ stretching vibrations as a quantitative measure of the equatorial bond covalency in uranyl complexes: a quantum-chemical investigation[J]. Inorg Chem, 2016, 55(2): 573-583.

[19] Ruipérez F, Danilo C, Real F, et al. An *ab initio* theoretical study of the electronic structure of $UO_2^+$

and $[UO_2(CO_3)_3]^{5-}$[J]. J Phys Chem A, 2009, 113(8): 1420-1428.

[20] Páez-Hernández D. Predicting the electronic structure and magnetic properties of $UO_2^+$, $UO_2(CO)_5^+$ and $UO_2(Ar)_5^+$ using wavefunction based methods[J]. J Electron Spectrosc Relat Phenom, 2014, 197: 1-6.

[21] Zhao J, Chi C X, Meng L Y, et al. Cis- and trans-binding influences in $[NUO\cdot(N)_2)_n]^+$[J]. J Chem Phys, 2022, 157(5): 054301.

[22] Marks J H, Rittgers B M, Van Stipdonk M J, et al. Photodissociation and infrared spectroscopy of uranium-nitrogen cation complexes[J]. J Phys Chem A, 2021, 125(33): 7278-7288.

[23] Haiges R, Vasiliu M, Dixon D A, et al. The uranium(Ⅵ) oxoazides $[UO_2(N_3)_2\cdot CH_3CN]$, $[(bipy)_2(UO_2)_2(N_3)_4]$, $[(bipy)UO_2(N_3)_3]^-$, $[UO_2(N_3)_4]^{2-}$, and $[(UO_2)_2(N_3)_8]^{4-}$[J]. Chem-Eur J, 2017, 23(3): 652-664.

[24] Wang Y T, Han C C, Fei Z J, et al. Probing the hydrogen bonding in microsolvated clusters of $Au_{1,2}^-(solv)_n$ ($solv=C_2H_5OH$, $n$-$C_3H_7OH$; $n$=1-3 for $Au^-$; $n$=1 for $Au_2^-$)[J]. J Phys Chem A, 2020, 124(27): 5590-5598.

[25] Frisch M J, Trucks G W, Schlegel H B, et al. Gaussian 09, Revision A. 1[R]. Wallingford, CT: Gaussian, Inc, 2009.

[26] Becke A D. Density-functional thermochemistry Ⅲ: the role of exact exchange[J]. J Chem Phys, 1993, 98(7): 5648-5652.

[27] Dunning T H. Gaussian basis sets for use in correlated molecular calculations Ⅰ: the atoms boron through neon and hydrogen[J]. J Chem Phys, 1989, 90(2): 1007-1023.

[28] Peterson K A. Correlation consistent basis sets for actinides Ⅰ: the Th and U atoms[J]. J Chem Phys, 2015, 142(7): 074105.

[29] Vasiliu M, Peterson K A, Gibson J K, et al. Reliable potential energy surfaces for the reactions of $H_2O$ with $ThO_2$, $PaO_2^+$, $UO_2^{2+}$, and $UO_2^+$[J]. J Phys Chem A, 2015, 119(46): 11422-11431.

[30] Lu T, Chen F W. Multiwfn: a multifunctional wavefunction analyzer[J]. J Comput Chem, 2012, 33(5): 580-592.

[31] Weinhold F, Landis C R, Glendening E D. What is NBO analysis and how is it useful? [J]. Int Rev Phys Chem, 2016, 35(3): 399-440.

[32] Real F, Vallet V, Marian C, et al. Theoretical investigation of the energies and geometries of photoexcited uranyl(Ⅵ) ion: a comparison between wave-function theory and density functional theory[J]. J Chem Phys, 2007, 127(21): 214302.

[33] Vallet V, Schimmelpfennig B, Maron L, et al. Reduction of uranyl by hydrogen: an *ab initio* study[J]. Chem Phys, 1999, 244(2-3): 185-193.

[34] Servaes K, Hennig C, Van Deun R, et al. Structure of $[UO_2Cl_4]^{2-}$ in acetonitrile[J]. Inorg Chem, 2005, 44(22): 7705-7707.

[35] Sornein M O, Mendes M, Cannes C, et al. Coordination environment of $[UO_2Br_4]^{2-}$ in ionic liquids and crystal structure of $[Bmim]_2[UO_2Br_4]$[J]. Polyhedron, 2009, 28(7): 1281-1286.

[36] Vallet V, Wahlgren U, Schimmelpfennig B, et al. The mechanism for water exchange in $[UO_2(H_2O)_5]^{2+}$ and $[UO_2(oxalate)_2(H_2O)]^{2-}$, as studied by quantum chemical methods[J]. J Am Chem Soc, 2001, 123(48): 11999-12008.

[37] Ricks A M, Gagliardi L, Duncan M A. Infrared spectroscopy of extreme coordination: the carbonyls of $U^+$ and $UO_2^+$[J]. J Am Chem Soc, 2010, 132(45): 15905-15907.

[38] Wang X F, Andrews L, Li J, et al. Significant interactions between uranium and noble-gas atoms: coordination of the $UO_2^+$ cation by Ne, Ar, Kr, and Xe atoms[J]. Angew Chem Int Ed, 2004, 43(19): 2554-2557.

[39] Andrews L, Wang X F, Gong Y, et al. Infrared spectra and electronic structure calculations for NN complexes with U, UN, and NUN in solid argon, neon, and nitrogen[J]. J Phys Chem A, 2014, 118(28): 5289-5303.

[40] Andrews L, Wang X F, Gong Y, et al. Infrared spectra and electronic structure calculations for the $NUN(NN)_{1-5}$ and $NU(NN)_{1-6}$ complexes in solid argon[J]. Inorg Chem, 2013, 52(17): 9989-9993.